A Technical Feasibility of Aqueous Aerosol Generation Based on the Flashing Jet: Effects of Overheat Degree, Jetting Rate, Jetting Volume, and Liquid Type

Qi-Wen Zheng[1,#] Li-Jia Yuan[2,#] Jian Wang[1*]

[1] National Advance Medical Engineering Research Center, China State Institute of Pharmaceutical Industry Co., Ltd., Shanghai, People's Republic of China
[2] Center for Drug Evaluation, National Medical Products Administration, Beijing, People's Republic of China

Address for correspondence Jian Wang, PhD, National Advance Medical Engineering Research Center, China State Institute of Pharmaceutical Industry Co., Ltd., 285 Gebaini Road, Shanghai 201203, People's Republic of China (e-mail: wangjian11@sinopharm.com).

Pharmaceut Fronts 2023;5:e175–e186.

Abstract

A previously established flashing jet inhaler prototype (FJ prototype) can produce an aqueous aerosol but cannot steadily provide inhalable aerosol (2–5 μm). This study aims to optimize the atomization performance of the FJ prototype and generate inhalable aqueous aerosols. The effects of overheat degree, jetting rate, jetting volume, and liquid type on atomization performance were assessed by determining output aerosol's mass median aerodynamic diameter (MMAD) and aerodynamic particle size distribution. Drug distribution of active ingredients in different liquid types was also measured. A Pari nebulizer was used as a reference device. Our data suggested that MMAD is negatively correlated with the overheat degree and jetting rate, but has no significant relationship with the jetting volume. The effect of jetting rate is weaker than that of the overheat degree. When normal saline was used as the atomization liquid, output aerosol's MMAD at the FJ prototype and Pari nebulizer were 1.98 ± 0.18 and 2.50 ± 0.81 μm, respectively. The addition of a surfactant significantly decreases MMAD both in solution and in suspension, but the suspended particles had no effect on the residual level and atomization performance of the FJ prototype. When ventolin was used as the atomization liquid, the MMAD of the FJ prototype and Pari nebulizer was 2.1 ± 0.2 and 1.7 ± 0.2 μm, respectively, while the fine particle dosage (FPD) in percent of the nominal dose (%ND) was 50.4 ± 3.1 and 53.1 ± 7.2%, respectively. When pulmicort respules was used as the atomization liquid, the MMAD of the FJ prototype and Pari nebulizer was 2.5 ± 0.5 and 4.6 ± 0.2 μm respectively, while the FPD (%ND) was 30.1 ± 5.6 and 58.6 ± 5.1%, respectively. The FJ prototype not only delivers inhalable aqueous aerosol but also has a potential advantage in the atomization of suspension or poorly soluble drugs.

Keywords
- flashing jet
- FJ prototype
- atomization performance
- mass median aerodynamic diameter

Introduction

Inhalation is an administration method in which aerosolized medications are inhaled into the respiratory tract and further reach the pulmonary system for topical or systemic

[#] *These authors contributed equally to this work.*

received
February 3, 2023
accepted
July 11, 2023
article published online
August 18, 2023

DOI https://doi.org/10.1055/s-0043-1772193.
ISSN 2628-5088.

Georg Thieme Verlag KG, Rüdigerstraße 14, 70469 Stuttgart, Germany

applications.[1] It is the recommended administration method for asthma and chronic obstructive pulmonary disease.[2] Compared with oral administration, inhalation drug delivery offers several advantages including lower delivery doses, reduced incidence of systemic side effects, faster onset of action, and improved bioavailability.[2–4]

An inhalation medication is atomized and delivered through an aerosol device. There are three main types of aerosol devices: pressurized metered dose inhaler, dry powder inhaler, and nebulizer, which include jet nebulizer, ultrasonic nebulizer, and vibration mesh nebulizer. Besides, emerging inhaler and nebulizers have been investigated, such as vortex nozzle inhaler, plume-control inhaler, air classifier inhaler, turbulent flow inhaler, flutter inhaler, thermostat jet nebulizer, surface acoustic wave microfluidic atomizer, condensational growth capillary aerosol generator, and on-chip electrohydrodynamic atomizer.[5–11]

Critical factors such as dosage level, drug efficacy, drug safety profile, patient age, disease severity, ease of administration, and cost should be considered when selecting a suitable inhaler or nebulizer for a patient.[12–14] An ideal inhaler generally provides better usability, lower spray velocity, longer spray duration, higher fine-particle fraction, and better drug utilization.[15] Currently, these attributes are largely showcased by Respimat soft mist inhaler, but its unique uniblock component restricts the delivery volume to 15 µL, which considerably diminishes the drug delivery capacity.[16–19] Additionally, drugs with poor solubility are unsuitable for Respimat soft mist inhaler. Therefore, a novel inhaler that can produce a soft mist with higher atomization volume and better support for poorly soluble drugs will be a good complement to current inhalers.

Flashing is an instantaneous boiling phenomenon that happens when the external pressure of a liquid drops below its saturated vapor pressure.[20] Under such circumstances, the liquid is "overheated", and boiling happens. This process is quicker and more violent than normal ebullition. When flashing liquid flows through an orifice, a two-phase bubble flow is created. The rapid expansion of the bubble shatters the liquid flow and aerosol spray is generated.[20–24]

When the flashing happens inside or before the orifice of an atomizer, a flash atomization happens.[20,25] Spray ejected by the flash atomization has high controllability on droplet size and distribution pattern. Therefore, flash atomization is widely applied in several industrial applications such as coating, cooling, dehydration, desalination, aerospace, and pharmaceutical.[26] When the flashing happens after the orifice, a flashing jet is generated.[27] Aerosol characteristics of the flashing jet, such as the velocity, spray angle, and droplet size distribution, can be used to calculate the jetting rate and orifice diameter of the jet.[28,29] Therefore, this flashing form receives considerable attention in heavy industries as a measurable feature to estimate the leakage rate of high-pressure vessels or circulation loops for risk assessment and hazard management.

Liquid pressure, temperature, overheating degree, surface tension, and nozzle geometry are critical factors that determine the droplet size and distribution of output aerosol at the flashing jet.[27,28,30–32] Currently, multiple theoretical formulas can be used to predict droplet size changes under different parameter conditions.[20,33,34] Theoretical droplet size d_d can be calculated through Equation (1)[21]:

$$d_d = \begin{cases} 1.89 d_f \sqrt{1 + 3\dfrac{We_{Lf}^{0.5}}{Re_{Lf}}}, & if\left(We_{LF} < 10^6 Re_{Lf}^{-0.45} \; and \; T_0 < 1.11 T_v^{sat}\,(Pa)\right) \\ \dfrac{\sigma_L We_{crit}}{u_f^2 \rho_a}, & else. \end{cases} \tag{1}$$

Herein, the critical Weber number We_{crit} was 12.5, which is recommended by a previous study.[27] The liquid Reynolds number and the liquid Weber number are defined as Equation (2):

$$Re_{Lf} = \frac{\rho_L u_f d_f}{\mu_L}, \; We_{Lf} = \frac{\rho_L u_f^2 d_f}{\sigma_L}. \tag{2}$$

Where d_f is the initial diameter of the jet, ρ_L is the density of the liquid, u_f is the initial speed of the jet, μ_L is the viscosity coefficient of the liquid, and σ_L is the surface tension coefficient of the liquid.

However, limited experiments are available that establish a direct correlation between these definitions and practical usage. Therefore, a new correlation derived from experimental data is being employed. The droplet diameter can be calculated based on the orifice diameter using the following Equation (3)[21,35]:

$$d_d = \begin{cases} 64.73 We_{Lo}^{-0.533} Re_{Lo}^{-0.014} \left(\frac{L}{d_0}\right)^{0.114} d_0, & \Delta T < start\ point. \\ d_{str} - 2.4\Delta T, & start\ point < \Delta T \le end\ point. \\ d_{end} - 0.1\Delta T, & end\ point < \Delta T. \end{cases} \tag{3}$$

Where d_O is the orifice diameter, d_{str} is the droplet diameter at the start point when the flashing transition begins, and d_{end} is the droplet diameter at the endpoint when the flashing transition finishes. The start and end temperatures of this flashing transition process can be calculated based on the criteria given in Equation (4):

$$\begin{cases} start\ point: Ja\emptyset = 55We_v^{-1/7} \\ end\ point: Ja\emptyset = 150We_v^{-1/7} \end{cases}, \quad with \begin{cases} \emptyset = 1 - e^{-2300(\rho_v/\rho_L)} \\ We_v = \dfrac{\rho_v u_O^2 d_O}{\sigma_L} \\ Ja = \dfrac{C_{pL}\Delta T}{h_{fg}} \times \dfrac{\rho L}{\rho v} \end{cases}. \tag{4}$$

According to the current flashing theory, obtaining aqueous aerosol particles with diameters less than 10 µm is achievable for the flashing atomization but difficult for the flashing jet.[21,25,27,29,36,37] Although flashing atomization is already used in spray dying applications to generate super-fine droplets (< 1 µm) for pharmaceutical dry powder production,[34] it is rarely used to generate inhalable droplets (2–5 µm) for drug inhalation application. This may be because the high-pressure differential (> 400 kPa), large expansion chamber volume, and high energy supply requirements limit the feasibility of miniaturizing a flashing atomizer into handheld size,[30] which is a basic usability requirement for inhalers. On the other hand, current theoretical and experimental data of the flashing jet focus on large orifice diameter (> 1 mm), high pressure (> 300 kPa), or high flow rate (> 100 mL/s).[35–37] The possibility and methodology to generate inhalable aerosols remain unknown when the flashing jet is produced through an inhaler nozzle setting.

In the preliminary work of this study, a flashing jet inhaler prototype (FJ prototype) was established, which produced small droplets (< 10 µm) with a small orifice (0.4 mm) and lower liquid pressure (150 kPa) in a single spray (50 µL). The atomization mechanism of the FJ prototype dose relied on the propellant, and the atomization performance is not affected by the inhalation flow. Additionally, the spray speed was relatively slow, and the spray duration could be adjusted in the FJ prototype. The FJ prototype holds the potential for improving drug delivery efficiency and usability. However, a significant proportion of large droplets remained in the delivered aerosol, making it unsuitable for inhalation administration. Therefore, further optimization of atomization performance is necessary for the FJ prototype.

The study aims to investigate the feasibility of using the current flashing theory to optimize the atomization performance of the FJ prototype and generate inhalable aqueous aerosols, and the factors that influence the flashing jet appearance are studied, including the overheat degree, jetting rate, jetting volume, and liquid type. The mass median aerodynamic diameter (MMAD) and aerodynamic particle size distribution (APSD) of output aerosol are used to compare the effects of these factors on atomization performance. Moreover, drug distribution is measured to evaluate the drug delivery capacity when active ingredients are included in different liquid types.

Material and Method

Instrument and Materials

The instrument used in the study were: high-performance liquid chromatography (HPLC, LC-20AT Shimadzu, Japan), aerodynamic particle sizer (APS) model 3321 (TSI Inc., Minnesota, United States), impactor inlet for pharmaceutical research (IIPR) model 3306 (TSI Inc., Minnesota, United States), vacuum pump (2XZ(s)-2, SH-Drying Vacuum & Lighting Equipment Co., Ltd., Shanghai, China), air flow meter LZB-10 (QF-meter, China), glass microfiber filter (Whatman GF/F, Maidstone, Kent, United Kingdom), analytical balance XS205DU (Mettler Toledo Ltd., Leicester, United Kingdom), Pari nebulizer, and FJ prototype.

Materials and chemical reagents used in the study were: methanol (16891140) and acetonitrile (Z2611440), obtained from CNW Technologies GmbH, Germany; phosphoric acid (20120920), sodium dihydrogen phosphate dehydrate (20170209), sodium dihydrogen phosphate (20170417), and sodium chloride (20161207), obtained from Sinopharm Chemical Reagent Co., Ltd., Shanghai, China. Salbutamol sulfate (cpc-007–1712005, SPH Sine Pharmaceutical Laboratories Co., Ltd., Shanghai, China), salbutamol sulfate solution (SAL) for inhalation (ventolin [VEN], 5 mL/mL, C713079, GlaxoSmithKline, United Kingdom), budesonide (BD131102, Hubei Gedian Humanwell Pharmaceutical Co., Ltd., Hebei, China), and budesonide suspension (BUD) for inhalation (pulmicort respules [PUL]; 2 mL:1 mg, 318703, Astra-zeneca, United States). Methanol and acetonitrile were of chromatographic grade, and all other reagents were of analytical grade. Purified water was used throughout the study.

FJ Prototype

The FJ prototype consists of an atomization block, temperature control module, pressure–volume control module, and liquid pool (►**Fig. 1A**). The temperature control module contains a thermistor temperature sensor, a 25 W ceramic heater, and a temperature controller. The pressure–volume control module contains a metering pump, a pressure sensor, an actuation pusher, and a pressure chamber. Moreover, this module connects the liquid pool and the atomization block. The whole prototype is powered by a 50 W DC power.

The atomization process of the FJ prototype includes two steps: preparation and actuation. In the preparation stage, a certain amount of liquid is extracted from the liquid pool and pumped into the pressure chamber. Next, the chamber pressure is raised above the saturation pressure of the target overheating temperature. Additionally, the pressure chamber is heated to the overheating temperature. The chamber

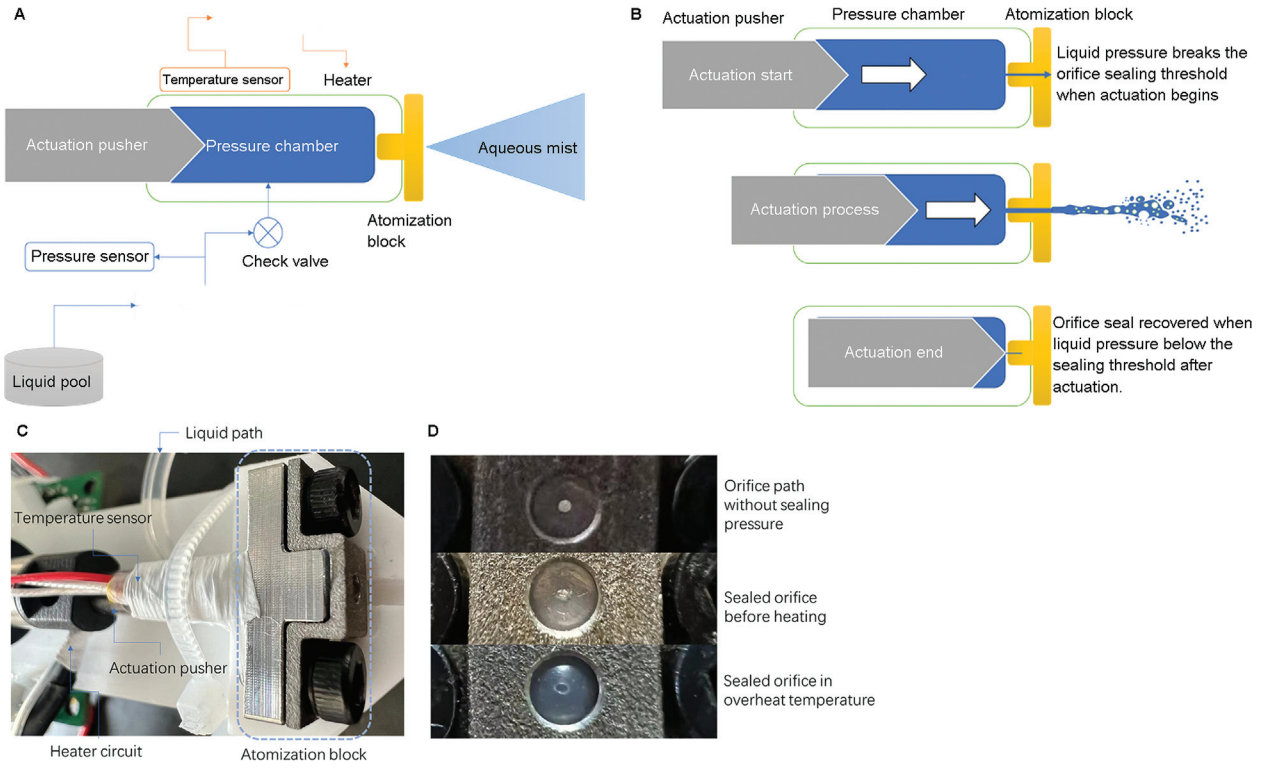

Fig. 1 Diagrammatic view of the FJ prototype. (**A**) Prototype composition; (**B**) actuation process; (**C**) partial photo of atomization block; (**D**) top view of the atomization block under different conditions. FJ, flashing jet inhaler.

pressure is adjusted by the position of the actuation pusher and maintained by a check valve outside the chamber. The heating and stabilization process is controlled by the temperature control loop between the ceramic heater and the temperature sensor.

During the actuation, the pusher is inserted into the chamber to further increase the liquid pressure. When the liquid pressure is higher than the orifice sealing threshold, the orifice opens releasing overheated liquids as a flashing jet (►**Fig. 1B**). The jetting rate and duration are controlled by the insertion rate of the pusher. The orifice sealing threshold is controlled by the locking strength of the atomization block and the orifice diameter.

APSD and MMAD Measurement

The APSD of the delivered aerosol was measured by the APS based on the time of flight (TOF) analysis. The IIPR, which has a United States Pharmacopeia/European Pharmacopeia (USP/Ph Euro) inlet and an APS sampling probe, was integrated with the APS.

The background flow rate of the APS/IIPR system was set as 28.3 L/min, while the sampling flow rate of the APS probe was set as 0.062 L/min with a sampling pressure of 1.2 cm in the water manometer (approximately 117.68 Pa). As a result, 0.2% of the delivered aerosol that penetrated through the USP/Ph-Euro inlet was extracted as the initial sample. Filter makeup air was mixed with the initial sample twice before it enters the TOF spectrometer in APS, which leads to the total dilution rate of the delivered aerosol being 1:400.

Aerosol Instrument Manager (version 7.3.0.0, TSI Inc., Minnesota, United States) was used for data calculation and display. The sampling mode of aerosol was settled as summing and the measured results of APSD were displayed as channel date. Stokes correction scatter mode was not applied. Dilution/efficiency file <00400to1.e21> was used as the data compensation algorithm. The measuring range of MMAD was 0.523 to 20 µm.

Dosage Measurement

The USP throat, 4.7 µm single-stage impactor, and outlet filter in the APS/IIPR system were used to measure the drug dosage of the delivered aerosol. After atomization, the atomization block of the FJ prototype, connecter, USP throat, and impact plates were washed by the mobile phase. Thereinto, the lotion of the atomization block was considered as the device residual dosage sample, the lotions of connecter and USP throat were merged as throat residual dosage sample, and the lotions of impact plates were merged as the large particle dosage (LPD) sample. The glass microfiber filter, which was loaded on the outlet holder in IIPR, was soaked and ultrasonicated for 30 minutes in the mobile phase. Subsequent filtration after 0.22 µm filtration was used as fine particle dosage (FPD) samples. All samples were measured by the HPLC.

Chromatographic Conditions

For salbutamol sulfate, a Kromasil C18 (4.6 mm × 250 mm, 5 µm) column was used with the mobile phase

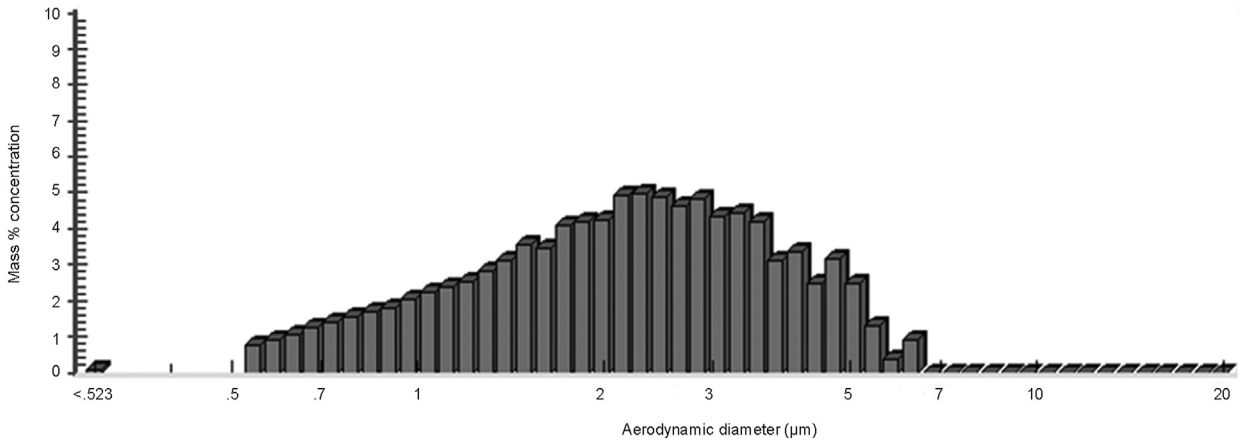

Fig. 2 APSD of NS at the Pari nebulizer. APSD, aerodynamic particle size distribution; NS, normal saline.

comprising phosphate buffer solution–methanol (85:15, v/v), detection wavelength of 276 nm, flow rate of 1.0 mL/min, injection volume of 20 μL, and column temperature of 35°C.

For budesonide assessment, an Inertsil ODS-SP C18 (4.6 mm × 250 mm, 5 μm) column was used with the mobile phase consisting of phosphate buffer solution–acetonitrile (58:42, v/v), detection wavelength of 246 nm, flow rate of 1.0 mL/min, injection volume of 20 μL, and column temperature of 35°C.

Statistical Analysis

Data were managed and analyzed with the SPSSAU data analytics platform. Data were expressed in the form: mean ± standard deviation. One-way ANOVA (analysis of variance) was employed to evaluate data dependency. A statistically significant difference was set as the *p*-value is less than 0.05.

Results

Reference Output

The APS/IIPR system was used to measure the APSD and MMAD of output aerosol. However, the potential shrinking caused by the sampling flow results in deviations from the original droplet diameter.[38,39] Droplet sizes determined by the APS/IIPR system alone are not suitable to evaluate

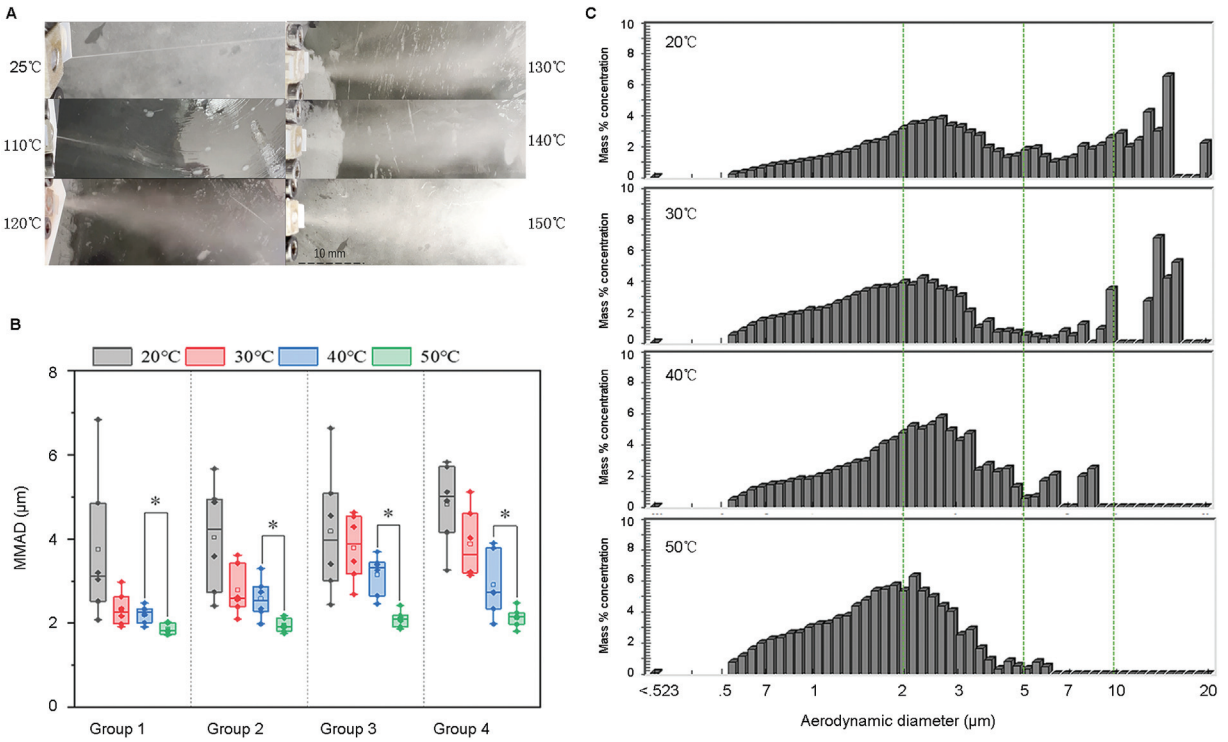

Fig. 3 (**A**) FJ prototype output at different temperatures. (**B**) Atomization performance at different overheat degrees ($n = 6$). $^{*}p < 0.05$. (**C**) APSD of NS at different overheat degrees. APSD, aerodynamic particle size distribution; FJ, flashing jet inhaler; NS, normal saline.

the atomization performance. Among the numerous jet nebulizers, the Pari nebulizer is widely recognized for its atomization performance. The Pari nebulizer was used as a reference device because it produces aqueous aerosol, similar to the output of the FJ prototype. The MMAD and APSD of aerosol output at 60 seconds of the Pari nebulizer were used to assess the atomization performance of the FJ prototype.

Normal saline (NS) was nebulized by the Pari nebulizer with a 2 mL initial filling volume. The MMAD of its aerosol output in 60 seconds was 2.50 ± 0.81 μm ($n = 6$). The APSD is shown in ►**Fig. 2**.

Overheat Degree

The overheat degree $\triangle T$ is the difference between the liquid temperature (T_L) and the liquid boiling point ($T_{boiling}$) corresponding to the current ambient temperature, according to Equation (5):

$$\Delta T = T_L\text{-}T_{boiling} \quad (5)$$

A higher overheat degree leads to a more drastic flashing process, whereas it also leads to lower liquid surface tension and viscosity. With increasing overheat degrees, three stages may exist: (1) jetting stage, where no flashing happens or the flashing is not strong enough to break the jet; (2) rupturing stage, where flashing is strong enough to break the jet into aerosol; (3) full flashing stage, where flashing disintegrates the jet violently near the nozzle. Multiples overheat degrees of 10, 20, 30, and 50°C were used as flashing conditions to evaluate the output changes of the FJ prototype.

NS was jetted by the FJ prototype in a jetting volume of 40 μL, a jetting rate of 20 μL/s, a jetting pressure of 150 kPa, and a jetting duration of 2 seconds. Atomization output at different temperatures is shown in ►**Fig. 3A**.

No data were obtained at the 10°C overheat degree because the flashing was not strong enough to break the jet into an aerosol. Moreover, two FJ prototype devices were used in the test, while the second one was repeatedly tested three times on other days to validate the repeatability and reproducibility.

Measured MMAD decreased with increased overheat degree. Significant differences were found between the 40 and 50°C overheat degrees in all test groups (►**Fig. 3B**). APSDs at different overheat degrees are shown in ►**Fig. 3C**.

Jetting Rate

The jetting rate influences the initial velocity of the flashing jet. The interaction of air and jet directly causes the disturbance in

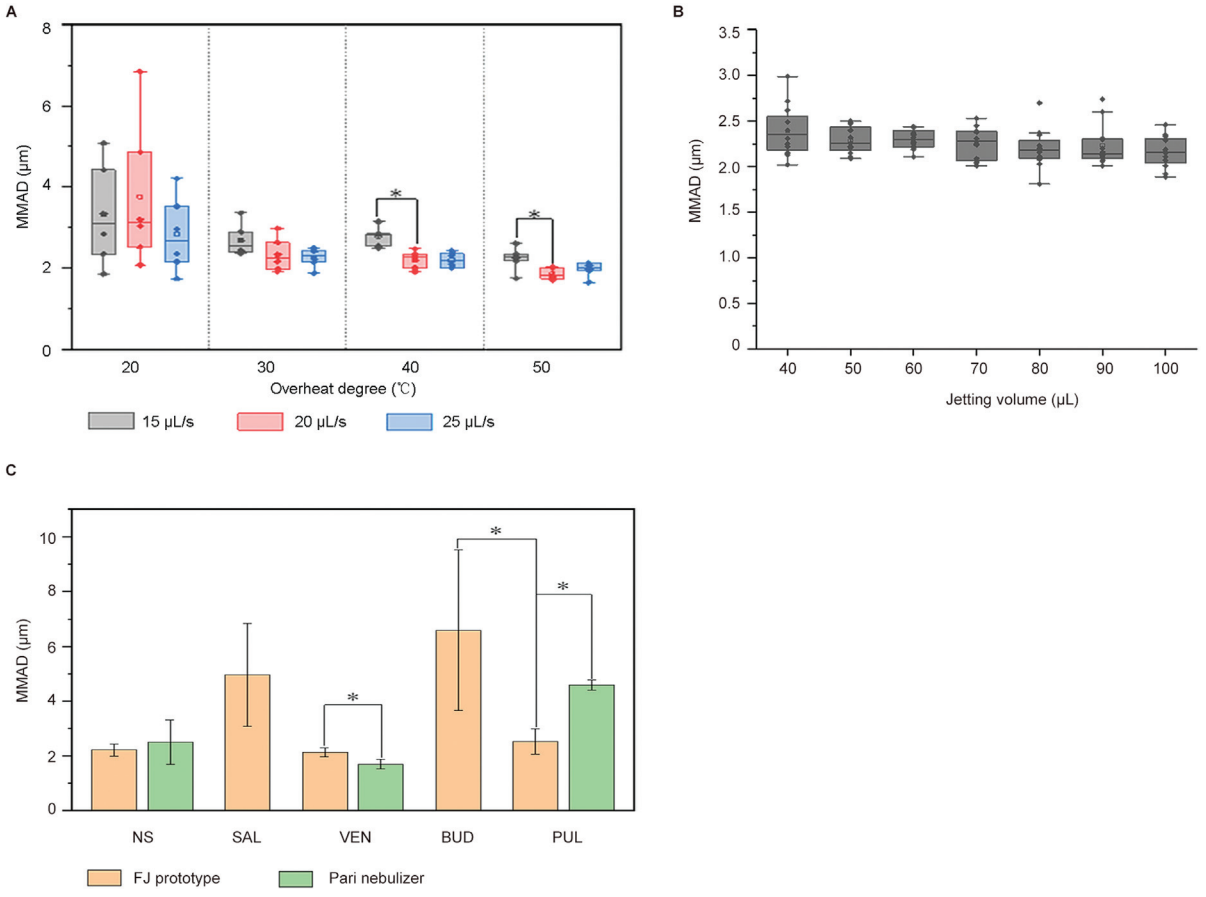

Fig. 4 (**A**) Atomization performance at different jetting rates ($n = 6$). *$p < 0.05$. (**B**) MMAD of delivered aerosol at different jetting volumes. (**C**) MMAD of different atomization liquids at FJ prototype and Pari nebulizer. *$p < 0.05$. FJ, flashing jet inhaler; MMAD, mass median aerodynamic diameter.

the air–liquid interface, which weakens the constraint effect of surface tension. Therefore, a higher jetting rate may improve the atomization performance in the same flashing strength.

NS was used as the atomization liquid, the jetting volume was 40 µL, and jetting rates of 15, 20, and 25 µL/s were evaluated. Besides, the effect of jetting rate in different overheat degrees was assessed by determining MMAD and APSD of the FJ prototype at 20, 30, 40, and 50°C.

Our data showed that at low overheat degrees (20 and 30°C), the aerosol MMAD tends to decrease with the increase of jetting rate, but the difference is not significant. At high overheat degrees (40 and 50°C), the aerosol MMAD decreased significantly between the injection rate of 15 and 20 µL/s, but did not decrease further when the jetting rate increased to 25 µL/s (►**Fig. 4A**). APSDs for different jetting rates at 20 and 50°C overheat degrees are shown in ►**Fig. 5A**.

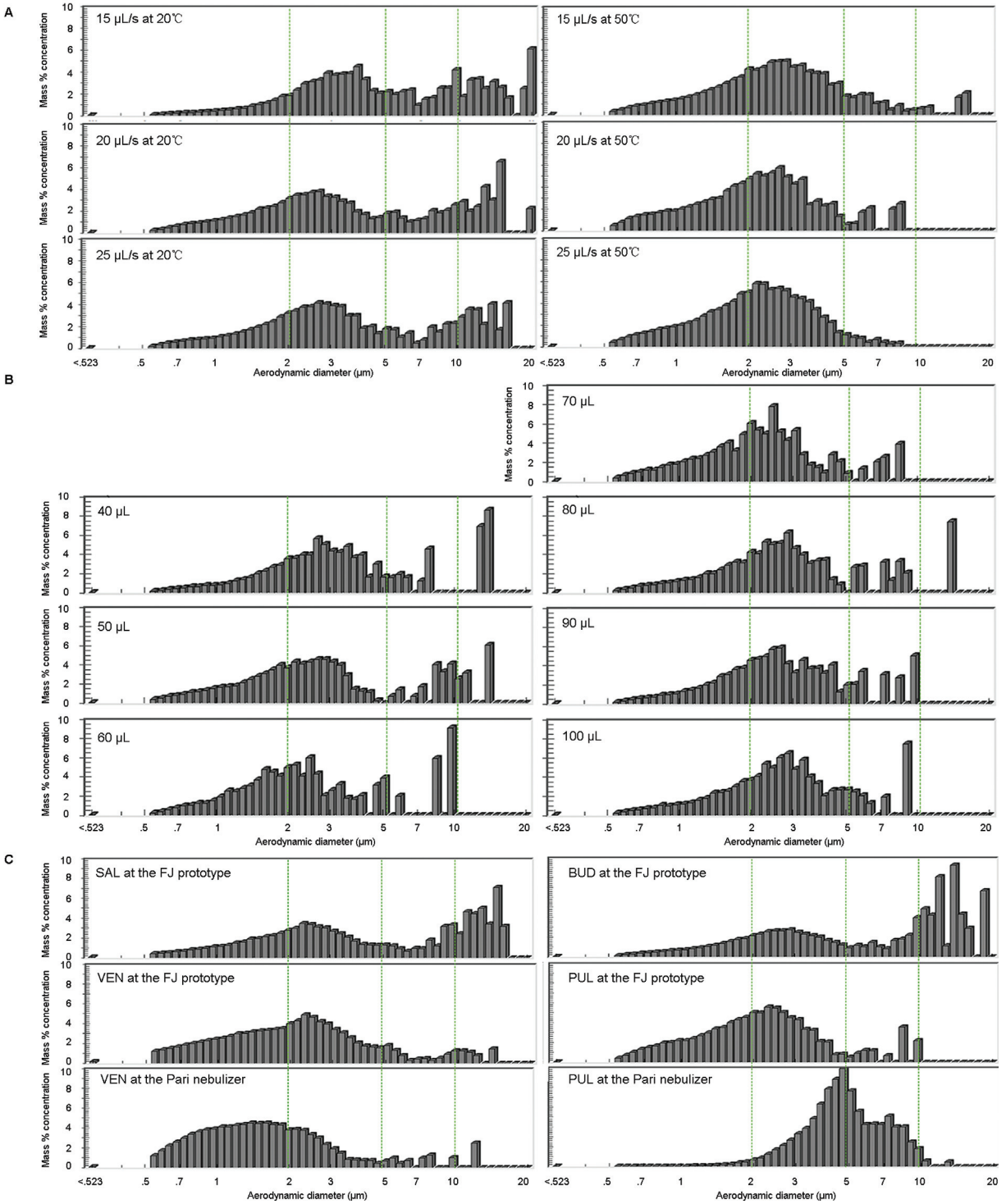

Fig. 5 (**A**) APSD of normal saline at different jetting rates; (**B**) APSD of normal saline at different jetting volumes; (**C**) APSD of different atomization liquids at FJ prototype and Pari nebulizer. APSD, aerodynamic particle size distribution; FJ, flashing jet inhaler.

Table 1 Results of dosage measurements

	FJ prototype				Pari nebulizer	
	SAL	VEN	BUD	PUL	VEN	PUL
Device (%ND)	19.9 ± 4.5	22.0 ± 4.3	20.5 ± 8.2	25.1 ± 7.9	11.6 ± 7.7	9.2 ± 2.1
Throat (%ND)	34.3 ± 3.6	20.6 ± 3.3[a]	37.2 ± 11.5	36.4 ± 2.2	28.5 ± 5.6	27.2 ± 5.1
LPD (%ND)	26.0 ± 1.6	7.1 ± 2.9[a]	19.2 ± 9.6	8.4 ± 2.1	6.9 ± 1.2	25.0 ± 6.4
FPD (%ND)	19.7 ± 1.9	50.4 ± 3.7[a]	23.1 ± 6.6	30.1 ± 5.6	53.1 ± 7.2	38.6 ± 5.1
DD (%ND)	107.8 ± 8.0	97.7 ± 8.8	117.9 ± 10.1	89.9 ± 7.9	110.7 ± 6.0	99.5 ± 9.4
MMAD (μm)	4.9 ± 1.8	2.1 ± 0.2	6.6 ± 2.9	2.5 ± 0.5	1.7 ± 0.2	4.6 ± 0.2

Abbreviations: %ND, percent of the nominal dose; BUD, budesonide suspension; FJ, flashing jet inhaler; MMAD, mass median aerodynamic diameter; NS, normal saline; PUL, pulmicort respules; SAL, salbutamol sulfate solution; VEN, ventolin.
Note: Data were expressed as mean ± standard deviation of three parallels.
[a]Significant difference compared with SAL solution at FJ prototype.

Jetting Volume

The jetting volume and jetting rate determine the spray duration of one actuation. Moreover, larger volumes may lead to different pressure distributions in the pressure chamber, which may further influence the atomization performance of the FJ prototype.

For NS as the atomization liquid, an overheat degree of 40°C, a jetting rate of 20 μL/s, and jetting volumes of 40, 50, 60, 80, 90, and 100 μL were used as test conditions. The MMAD and APSD of the FJ prototype were measured to evaluate the effect of jetting volume.

The MMAD slightly decreased with increased jetting volume at the test condition, but no significant difference was found (►**Fig. 4B**). APSDs for different jetting volumes at 40°C overheat degree and 20 μL/s jetting rate are shown in ►**Fig. 5B**.

Atomization Liquid

The flashing behavior could be determined by the overheat degree, specific heat capacity, and vaporization latent heat of the liquid during jetting. Thereinto, the specific heat capacity and vaporization latent heat are influenced by the active ingredient and excipients in prescription.

NS, SAL, VEN, BUD, and PUL were used as the atomization liquid. Test conditions were set as follows: overheat degree, 40°C; jetting rate, 25 μL/s, and jetting volume: 50 μL. The atomization liquid was evaluated by determining the drug distribution and MMAD of the FJ prototype. Furthermore, VEN and PUL, atomized with a Part nebulizer, were used as reference groups. As shown in ►**Fig. 4C**, the MMAD of VEN and PUL at the FJ prototype was lower than those of SAL and BUD. The MMAD of VEN at the FJ prototype was significantly higher than that of the Pari nebulizer, while the MAMD of PUL at the FJ prototype was significantly lower than that of the Pari nebulizer. When the atomization liquid was NS, there is no significant difference between the FJ prototype and Pari nebulizer. Dosage measurement results of drug distribution are listed in ►**Table 1**, while the APSD of different liquids is shown in ►**Fig. 5C** below.

The normal dosage (ND) was calculated using the jetting volume and liquid concentration according to Equation (6):

$$ND = Atomized\ volume \times Liquid\ concentration \tag{6}$$

The ND at the FJ prototype was 250 μg for the SAL and VEN and 25 μg for the BUD and PUL, while at the Pari nebulizer was 800 and 80 μg for the VEN and PUL, respectively. Device (%ND) is the residual dosage proportion of the atomization block at the FJ prototype and the upper part of the nebulizer cup at the Pari nebulizer respectively. Throat (%ND) is the residual dosage proportion of connector and USP throat. LPD (%ND) and FPD (%ND) are the LPD proportion and FPD proportion, respectively. Delivered dosage (DD) is the sum of measured dosage, while DD (%ND) is the recovery rate of atomized dosage.

Discussion

Effect of Overheat Degree

The degree of overheat determines the boiling strength of the flashing jet, and a higher overheat degree leads to better atomization performance.[27] This factor has been extensively studied by various researchers, leading to the development of several empirical formulas that describe the relationship between the overheat degree and the mean droplet diameter of the output aerosol.[27,29,37]

Although the prediction results of particle size distribution are different in these formulas, it is recognized that there are three stages of size change trends as the overheat degree increases: mechanical breakup, transition, and fully flashing (►**Fig. 6**).[25,35,36] In the fully flashing stage, a fully flashed point is reached, beyond which there exists a cut-off value for the overheat degree. At this point, the reduction rate of particle size decelerates, and eventually, a constant value is achieved.

In this study, output aerosols of the FJ prototype at 20 to 40°C overheat degree belong to the transition stage, while the 50°C output belongs to the fully flashing stage (►**Fig. 3A**). As the overheat degree increased, the proportion of large droplets in the APSD rapidly decreased and almost

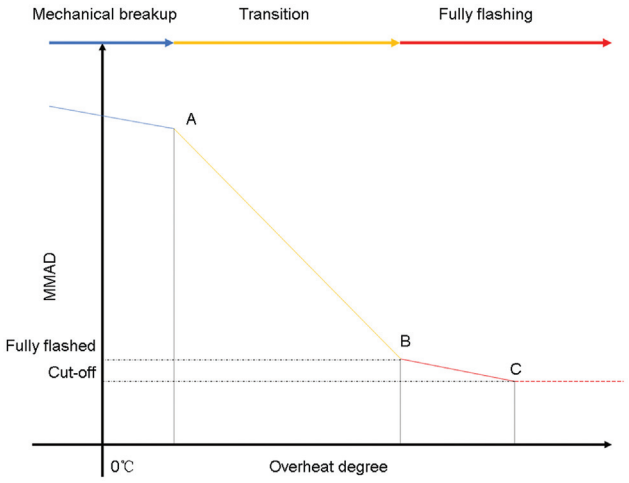

Fig. 6 Three changing stages of MMAD with increasing overheat degree. MMAD, mass median aerodynamic diameter.

disappeared at the fully flashing stage (►**Fig. 3C**). The disappearance of large droplets is the main cause of the MMAD reduction in the transition stage.

At low overheat degrees, a normal distribution of fine droplet sizes is observed. Following the increment of overheat degree, the proportion of the fine droplets is increased because large droplets are further broken into small droplets. The median of the fine droplet size is also decreased in this process. When the large droplets are gone, this shift becomes the dominant factor in MMAD change, which corresponds to the slow decline stage between the fully flashed and cut-off points (interval between point B and C). Droplet shrinkage caused by evaporation is the main cause of the change.[30] Due to the liquid's latent heat of vaporization approximately three orders of magnitude higher than the specific heat capacity, the residual heat after flashing breakup causes a minor change in droplet diameter.

The limitation of the evaporation rate is a possible cause of the cut-off value of MMAD (interval after point C). The humidity of the surrounding air of the aerosol in this stage is probably saturated due to the evaporation that happens in the flashing and large droplet breakup process. Hence, the evaporation rate is constrained to a minimum value. No evaporation would happen until additional saturated moisture content provided by the air convection is larger than the evaporation rate of the flashing process.

Effect of Jetting Rate and Volume

When the jetting rate increases, the influence on the flashing jet embodies in the increased jet speed and changes in pressure gradient within the orifice. A higher jet speed strengthens the air disturbance on the liquid jet, which produces smaller droplets after jet rupture.[40] This explains the shift of APSD at 50°C (►**Fig. 5A**). However, the turbulence rupture of liquid jet requires an extra jetting distance for distribution development.[41] In the flashing jet atomization process, flashing happens before the air disturbance is strong enough to influence the droplet production. In a low overheat degree, the shift of APSD is also observed, but large droplets caused by low flashing strength raised the MMAD (►**Fig. 5A**). Hence the effect of jetting rate on MMAD is weaker than the overheat degree.

The jetting rate is controlled by the advance rate of the pusher in the FJ prototype. Therefore, the change in jetting volume has limited impact on the jetting rate and atomization performance (►**Fig. 5B**). When the jetting rate is fixed, the jetting volume determines the spray duration of the FJ prototype.

A longer spray duration can lower the requirement on patient cooperation skill and improve the drug utilization for inhalers.[1] However, the prolonged duration can also reduce the inhalation administration effect because the aerosol delivered before or after the inspiration will be wasted. The duration of deep inspiration for healthy population is approximately 5 to 15 seconds, while a normal inspiration is approximately 1 to 2 seconds. However, the actual inspiration duration of a user is highly uncertain in clinical environments.[42–44]

An ideal spray duration should be able to complete the drug delivery within one inspiration. In consideration of the deviation caused by user skills, the spray duration of 1.5 to 2.5 seconds may be suitable for one deep inspiration to balance the benefit between the patient cooperation difficulty and delivery dosage loss.

When a high atomization volume is required, the spray duration can be controlled within the 1.5 to 2.5 seconds and limited the impact on atomization performance by adjusting the jetting rate at the FJ prototype. Consequently, there is a potential advantage at the FJ prototype on poorly soluble drug atomization, in which a high solvent volume is required to deliver adequate drug dosage.

Effect of Liquid Type

The MMAD of SAL is larger than that of NS at the FJ prototype. This change is directly related to the increment in large droplet ($>$ 5 μm) proportion in SAL (►**Figs. 2** and **5C**). The APSD change is probably caused by the rise of boiling point, which correspondingly decreased the overheat degree while the overheat temperature was not changed. The solution boiling point is related to its molality, and therefore, different overheat temperatures are required to obtain the same overheat degree in different liquid prescriptions.

A lower proportion of large droplets in the APSD of VEN is observed in the FJ prototype (►**Fig. 5C**) compared with SAL. This observation is attributed to the decrease in surface tension in VEN, which is caused by the presence of benzalkonium chloride in VEN prescription. In the same overheat degree, a lower surface tension leads to lower MMAD, consistent with other atomization mechanisms associated with liquid jets.[45–47]

Due to the presence of suspension, it is difficult to tell whether the fine particles of APSD was measured from aerosol droplets or powder particles when the BUD and

PUL were used. At the current stage, it is certain that the absence of large particles in ►**Fig. 5C** is also a result of a lower surface tension, which can be attributed to the inclusion of polysorbate 80 in the prescription of the PUL. Additionally, the significant difference in MMAD between BUD and PUL at the FJ prototype can likely be attributed to the use of micronized budesonide as the active ingredient in the PUL.

As a reference group, the APSD of VEN at the Pari nebulizer showed a normal distribution. Measured MMAD is approximately 1 μm lower than reported results in other studies.[48–50] This bias is consistent with existing studies comparing the measured results between APS, next-generation impactor (NGI), and Andersen cascade impactor (ACI).[39]

It is worth noting that the MMAD at the FJ prototype is smaller than the Pari nebulizer when PUL is used. A possible explanation of this difference is the potential promoting effect of suspended particles on flashing and droplet size reduction caused by evaporation. Another possible reason is that the atomization performance of the FJ prototype is less sensitive to the change of liquid viscosity. When stabilizing excipients in the PUL significantly affect the aerosol output at the Pari nebulizer, minimal changes are observed in the FJ prototype.

Device residual levels at the FJ prototype were higher than the Pari nebulizer. Adherence droplets around the orifice were observed in the beginning and ending stage of jetting at the FJ prototype. In the flashing process, these adherence droplets rapidly evaporated, leading to residual drug accumulation around the orifice. However, no significant difference of device residual level was found among the four atomization liquids at the FJ prototype (►**Table 1**), which indicates that liquid characteristics may have minimal impact on the device residual level.

The orifice structure is considered as a potential critical feature that may affect the device residual. On the one hand, the diameter, depth, and shape of the orifice determine the jet characteristic,[51] which further affect the adherence activity around the orifice. On the other hand, the outer surface shape around the orifice influences the evaporation and accumulation activity around the orifice. An improved orifice design may further decrease the device residual level of the FJ prototype. It is necessary to study the effects of orifice structures on atomization performance in future studies.

Research Limitations

The NGI or ACI was not used in this study for measuring the MMAD and FPD, because the NS was used throughout the study, which is not suitable for the impactor-based measurement of MMAD. The APS/IIPR system was used because it can measure droplet size without relying on HPLC, thus allowing for the measurement of NS aerosol.

It is important to note that the APS/IIPR is not widely accepted as a device for measuring MMAD, and the measured MMAD serves as a reference value. Considering the Pari nebulizer was used as the reference device, it is reasonable to conclude that the atomization performance of the FJ prototype is comparable to the Pari nebulizer, when the design of FJ prototype and the liquid prescription are further refined, the NGI or ACI would be better options for the MMAD measurement.

The Pari nebulizer was used as a reference device due to several factors. First, the Pari nebulizer produces an output of aqueous aerosol, which is similar to the output of the FJ prototype. Additionally, the Pari nebulizer allows for easy interchangeability of atomization liquids, making it a convenient choice for comparison. However, it is worth noting that the nebulizer operates as a continuous atomization device, which is different from the FJ prototype. In future studies, a more suitable option for comparison would be the soft mist inhaler Respimat. This is because it also delivers fine aqueous aerosol, and it shares similarities with the FJ prototype. Furthermore, the low delivery dosage limitation of Respimat aligns with one of its main drawbacks, whereas the FJ prototype potentially offers an advantage in high delivery doses.

The images of output aerosol at different temperatures (►**Fig. 3A**) were taken under normal laboratory conditions, the photographic environment was not fully controlled. When capturing images of aqueous aerosol, slight changes in camera settings and lightning conditions may significantly influence the image quality. Ideally the high-speed cameras in a controlled darkroom environment with a controlled near-end artificial light source should be used for image capture. The images presented in ►**Fig. 3A** can only be used for observing the phenomena rather than precise quantitative analysis.

Conclusion

In summary, the atomization performance of the FJ prototype is influenced by the overheat degree, jetting rate, and jetting liquid type, while the changes of jetting volume have a limited impact on aerosol output. The increase in overheat degree led to a decrease in MMAD, attributed to the enhanced flashing strength. Similarly, an increase in jetting rate resulted in a decrease in MMAD due to the increased air disturbance. The variation in atomization performance with different liquid types may be attributed to changes in boiling behavior.

For atomization liquids such as NS, VEN, and BUD, the FJ prototype can provide comparable output aerosol with the Pari nebulizer. This suggests the feasibility of generating aqueous aerosol for inhalation administration using the flashing jet method. Furthermore, the FJ prototype shows potential for delivering high solvent volumes or high-concentration suspensions in a single spray. Additionally, the flashing jet technique holds promise for atomizing suspensions or poor soluble drugs.

Conflict of Interest
None declared.

Acknowledgments
We thank SPH Sine Pharmaceutical Laboratories Co., Ltd., Shanghai, China and Hubei Gedian Humanwell Pharmaceutical Co., Ltd., Hubei, China for providing materials.

References

1 Anderson S, Atkins P, Bäckman P, et al. Inhaled medicines: past, present, and future. Pharmacol Rev 2022;74(01):48–118
2 Laube BL. The expanding role of aerosols in systemic drug delivery, gene therapy and vaccination: an update. Transl Respir Med 2014;2:3
3 Newman SP. Drug delivery to the lungs: challenges and opportunities. Ther Deliv 2017;8(08):647–661
4 Hickey AJ. Emerging trends in inhaled drug delivery. Adv Drug Deliv Rev 2020;157:63–70
5 de Boer AH, Hagedoorn P, Gjaltema D, Goede J, Frijlink HW. Air classifier technology (ACT) in dry powder inhalation Part 3. Design and development of an air classifier family for the Novolizer multi-dose dry powder inhaler. Int J Pharm 2006;310(1–2):72–80
6 Farkas D, Hindle M, Bonasera S, Bass K, Longest W. Development of an inline dry powder inhaler for oral or trans-nasal aerosol administration to children. J Aerosol Med Pulm Drug Deliv 2020; 33(02):83–98
7 Kakade PP, Versteeg HK, Hargrave GK, Genova P, Williams Iii RC, Deaton D. Design optimization of a novel pMDI actuator for systemic drug delivery. J Aerosol Med 2007;20(04):460–474
8 Shrewsbury SB, Armer TA, Newman SP, Pitcairn G. Breath-synchronized plume-control inhaler for pulmonary delivery of fluticasone propionate. Int J Pharm 2008;356(1–2):137–143
9 Ochowiak M, Kasperkowiak A, Doligalski M, et al. The thermostated medical jet nebulizer: aerosol characteristics. Int J Pharm 2019;567:118475
10 Qi A, Friend JR, Yeo LY, Morton DA, McIntosh MP, Spiccia L. Miniature inhalation therapy platform using surface acoustic wave microfluidic atomization. Lab Chip 2009;9(15):2184–2193
11 Frijlink HW, de Boer AH. Trends in the technology-driven development of new inhalation devices. Drug Discov Today Technol 2005;2(01):47–57
12 Geller DE. Comparing clinical features of the nebulizer, metered-dose inhaler, and dry powder inhaler. Respir Care 2005;50(10): 1313–1321, discussion 1321–1322
13 Respiratory protective devices for self-rescue-filter self-rescuer from carbon monoxide with mouthpiece assembly: I.S. EN 404:2005. Ireland: National Standards Authority of Ireland, 2005
14 McCarthy SD, González HE, Higgins BD. Future trends in nebulized therapies for pulmonary disease. J Pers Med 2020;10(02):37
15 Ari A, Fink JB. Recent advances in aerosol devices for the delivery of inhaled medications. Expert Opin Drug Deliv 2020;17(02): 133–144
16 Dalby R, Spallek M, Voshaar T. A review of the development of Respimat Soft Mist Inhaler. Int J Pharm 2004;283(1–2):1–9
17 Dalby RN, Eicher J, Zierenberg B. Development of Respimat(®) Soft Mist™ Inhaler and its clinical utility in respiratory disorders. Med Devices (Auckl) 2011;4:145–155
18 Ciciliani AM, Langguth P, Wachtel H. In vitro dose comparison of Respimat® inhaler with dry powder inhalers for COPD maintenance therapy. Int J Chron Obstruct Pulmon Dis 2017; 12:1565–1577
19 Ge Y, Tong Z, Li R, et al. Numerical and experimental investigation on key parameters of the Respimat® spray inhaler. Processes (Basel) 2021;9(01):44
20 Sher E, Bar-Kohany T, Rashkovan A. Flash-boiling atomization. Prog Energ Combust 2008;34(04):417–439
21 Witlox H, Harper M, Bowen P, Cleary V. Flashing liquid jets and two-phase droplet dispersion II. Comparison and validation of droplet size and rainout formulations. J Hazard Mater 2007;142 (03):797–809
22 Jiang X, Siamas GA, Jagus K, et al. Physical modelling and advanced simulations of gas–liquid two-phase jet flows in atomization and sprays. Prog Energ Combust 2010;36(02):131–167
23 Dumouchel C. On the experimental investigation on primary atomization of liquid streams. Exp Fluids 2008;45(03): 371–422
24 Li G, Li C. Experimental study on the spray steadiness of an internal-mixing twin-fluid atomizer. Energy 2021;226:120394
25 Bar-Kohany T, Levy M. State of the art review of flash-boiling atomization. At Sprays 2016;26(12):1259–1305
26 El-Fiqi AK, Ali NH, El-Dessouky HT, Fath HS, EI-Hefni MA. Flash evaporation in a superheated water liquid jet. Desalination 2007; 206(01):311–321
27 Brown R, York JL. Sprays formed by flashing liquid jets. AIChE J 1962;8(02):149–153
28 Calay RK, Holdo AE. Modelling the dispersion of flashing jets using CFD. J Hazard Mater 2008;154(1–3):1198–1209
29 Polanco G, Holdø AE, Munday G. General review of flashing jet studies. J Hazard Mater 2010;173(1–3):2–18
30 Fathinia F, Al-Abdeli YM, Khiadani M. Evaporation rates and temperature distributions in fine droplet flash evaporation sprays. Int J Therm Sci 2019;145:106037
31 Zhu X, Song Z, Pan X, Wang X, Jiang J. Critical superheat for flashing of superheated liquid jets. Ind Eng Chem Fundam 1986; 25(02):206–211
32 Zhu X, Song Z, Pan X, Wang X, Jiang J. Pressure-decay and thermodynamic characteristics of subcooled liquid in the tank and their interaction with flashing jets. J Hazard Mater 2019; 378:120578
33 Chen Q, Ja MK, Li Y, Chua KJ. Experimental and mathematical study of the spray flash evaporation phenomena. Appl Therm Eng 2018;130:598–610
34 Lobry E, Berthe JE, Spitzer D. Spray flash evaporation SFE process: identification of the driving parameters on evaporation to tune particle size and morphology. Chem Eng Sci 2021; 231:116307
35 Witlox HWM, Harper M, Oke A, et al. Sub-cooled and flashing liquid jets and droplet dispersion I. Overview and model implementation/validation. J Loss Prevent Proc 2010;23(06): 831–842
36 Cleary V, Bowen P, Witlox H. Flashing liquid jets and two-phase droplet dispersion I. Experiments for derivation of droplet atomisation correlations. J Hazard Mater 2007;142(03):786–796
37 Xiong P, He S, Qiu F, et al. Experimental and mathematical study on jet atomization and flash evaporation characteristics of droplets in a depressurized environment. J Taiwan Inst Chem Eng 2021;123:185–198
38 Mitchell JP, Nagel MW, Wiersema KJ, Doyle CC. Aerodynamic particle size analysis of aerosols from pressurized metered-dose inhalers: comparison of Andersen 8-stage cascade impactor, next generation pharmaceutical impactor, and model 3321 Aerodynamic Particle Sizer aerosol spectrometer. AAPS PharmSciTech 2003;4(04):E54
39 Harris JA, Stein SW, Myrdal PB. Evaluation of the TSI aerosol impactor 3306/3321 system using a redesigned impactor stage with solution and suspension metered-dose inhalers. AAPS PharmSciTech 2006;7(01):E20
40 Liu HM. Science and engineering of droplets: fundamentals and applications. Appl Mech Rev 2002;55(01):B16–B7
41 Hoeve W, Gekle S, Snoeijer J, et al. Breakup of diminutive Rayleigh jets. Phys Fluids 2010;22:122003
42 Anderson M, Collison K, Drummond MB, et al. Peak inspiratory flow rate in COPD: an analysis of clinical trial and real-world data. Int J Chron Obstruct Pulmon Dis 2021;16:933–943
43 Evans JA, Whitelaw WA. The assessment of maximal respiratory mouth pressures in adults. Respir Care 2009;54(10): 1348–1359
44 Westerdahl E, Gunnarsson M, Wittrin A, Nilsagård Y. Pulmonary function and respiratory muscle strength in patients with multiple sclerosis. Mult Scler Int 2021;2021:5532776

45 Gorokhovski M, Herrmann M. Modeling primary atomization. Annu Rev Fluid Mech 2008;40:343–366
46 Mc Callion ONM, Taylor KMG, Thomas M, Taylor AJ. The influence of surface tension on aerosols produced by medical nebulisers. Int J Pharm 1996;129(1–2):123–136
47 Steckel H, Eskandar F. Factors affecting aerosol performance during nebulization with jet and ultrasonic nebulizers. Eur J Pharm Sci 2003;19(05):443–455
48 Barry PW, O'Callaghan C. An in vitro analysis of the output of salbutamol from different nebulizers. Eur Respir J 1999;13(05): 1164–1169
49 Chang KH, Moon SH, Oh JY, et al. Comparison of salbutamol delivery efficiency for jet versus mesh nebulizer using mice. Pharmaceutics 2019;11(04):192
50 Zhou Y, Ahuja A, Irvin CM, Kracko DA, McDonald JD, Cheng YS. Medical nebulizer performance: effects of cascade impactor temperature. Respir Care 2005;50(08):1077–1082
51 Smyth H, Hickey AJ, Brace G, Barbour T, Gallion J, Grove J. Spray pattern analysis for metered dose inhalers I: orifice size, particle size, and droplet motion correlations. Drug Dev Ind Pharm 2006; 32(09):1033–1041